Journal of Solar Energy Research (JSER)

Journal homepage: www.jser.ut.ac.ir

Analysis and Implementation of Second-Order Step-Up Converter Using Winding Cross Coupled Inductors for Photovoltaic Applications

Ali Hussein Sachit[a], Bahdor Fani[b,c*], Majid Delshad[a], Ghazanfar Shahgholian[b,c*], Akbar Golsorkhi Esfahani[a]

[a]*Department of Electrical Engineering, Isfahan (Khorasgan) Branch, Islamic Azad University, Isfahan, Iran*
[b]*Department of Electrical Engineering, Najafabad Branch, Islamic Azad University, Najafabad, Iran*
[c]*Smart Microgrid Research Center, Najafabad Branch, Islamic Azad University, Najafabad, Iran*

ARTICLE INFO

Article Type:

Research Article

Received:01.04.2023
Accepted:31.01.2023

Keywords:
High boost converter
Voltage stress
Coupling inductors
Zero current switching

A B S T R A C T

One way to increase the voltage gain and reduce the voltage stress on the switch is by utilizing coupled inductors. However, a major drawback of this technique is the occurrence of voltage spikes on the switch, which are caused by the discharge of energy from the leakage inductance.

This paper proposes a zero current switching step-up converter to mitigate the voltage stress on the switch resulting from the high voltage gain of the converter. This enables the utilization of switches with lower drain-source resistance, leading to a more affordable price. The converter's auxiliary circuit requires minimal elements and does not require an additional switch, resulting in a straightforward control circuit. Another advantage of the converter is the transfer of energy from the auxiliary circuit to the output. Various operation modes of the proposed step-up converter have been investigated, and the converter's behavior has been simulated using PSpice software. To validate the accuracy of the analysis and simulation results, an 80W prototype has been implemented.

1. Introduction

Sunlight represents the largest renewable energy source on the planet, and there are two primary methods of harnessing this energy [1,2]: direct utilization of sunlight and its conversion into electricity through photovoltaic cells, as well as the

*Corresponding Authors Email: bahadorfani@gmail.com and shahgholian@iaun.ac.ir

Cite this article: Hussein Sachit, A., Fani, B., Delshad, M., Shahgholian, G., & Golsorkhi Esfahani, A. (2023). Analysis and Implementation of Second-Order Step-Up Converter Using Winding Cross Coupled Inductors for Photovoltaic Applications. Journal of Solar Energy Research, 8(2), 1516-1525.

DOI: 10.22059/jser.2023.357285.1291 DOR: 20.1001.1.25883097.2023.8.2.13.1

direct conversion of solar energy into other forms of energy [3,4].

One of the predominant approaches for utilizing solar energy is through the use of photovoltaic (PV) systems [5,6]. Employing these systems aids in environmental preservation, as photovoltaic electricity production has minimal detrimental effects on nature. In contrast to non-renewable and limited fossil fuels, solar energy stands as an unlimited and renewable resource [7,8].

However, photovoltaic cells often produce relatively low output voltages, necessitating the connection of multiple cells in series to achieve higher voltages [9,10]. Unfortunately, due to cell inconsistency and slight parameter variations, the overall power output of PV arrays is significantly diminished [11,12]. Alternatively, the parallel arrangement of PV cells exhibits greater efficiency than the series configuration. Nevertheless, the parallel structure generates lower voltages, ensuring the safety of electrical equipment in residential applications [13,14]. By combining solar cells in both series and parallel connections, a hybrid structure can be attained, which yields higher currents and voltages [15,16].

As the adoption of PV systems expands, it is crucial to address the impact on distribution network protection to prevent undesirable load shedding, grid equipment damage, and reduced reliability [17,18].

1.1. Literature review

So far, various studies have been conducted in the field of photovoltaic systems [1,2]. The effect of these types of systems has been investigated in different combinations and various methods have been presented to increase the benefit and control it [3,4].

Photovoltaic system control is presented as a distributed static compensator (DSTATCOM), with active current control and feedforward control loop in [5], where the PV system is independently converted to a DSTATCOM. It can provide ancillary services such as source current harmonic suppression, load reactive current compensation and power factor correction.

Power variations of a photovoltaic power plant on the frequency response of an islanded microgrid are investigated in [6], where the results show that the over-frequency phenomenon can be controlled by adjusting the PV inverters to achieve better reliability of the microgrid.

The application of a dynamic voltage restorer to enhance the power quality and improve the low voltage ride through capability of a three-phase medium-voltage network connected to a hybrid distribution generation system is proposed [7], which the photovoltaic plant and the wind turbine generator are connected to the same point of common coupling with a sensitive load.

A multi-objective approach for daily scheduling of microgrids contributing to higher penetration of photovoltaics is studied in [8], in which the existing control devices including distributed static synchronous compensator and under-load tap changer are integrated in volt/var control process.

The proposed approach in [9] is presented for the design of the boost converter for maximum power point tracking (MPPT), where the design is done according to the parameters of the PV module. The PV model is a single diode, and the hill-climbing MPPT algorithm using Simulink in MATLAB environment is used for simulation.

Mirtalaee and Amani-Nafchi [10], studied a DC-DC converter with a power of 200 watts and a high voltage gain is presented, which converts the output voltage of one to several solar cells that have a low DC voltage level to a higher and suitable DC voltage. Therefore, a non-isolated boost converter with coupled inductor is provided, and by reducing switching losses and conduction losses, it is tried to increase the efficiency of the converter.

A non-isolated step-up dc-dc converter with dual coupled inductors suitable for distributed generation applications is presented in [11], whereby implementing an input parallel connection in the proposed converter structure, the common input current will have low ripple. and therefore, a small capacitor filter is needed at the input. Also, active clamp circuits with a common snubber capacitor for the main switches are used in the proposed converter.

1.2. Main study and innovation

As stated, the output voltage of photovoltaic systems is low, and boost dc-dc converters with high gain and efficiency are needed to convert the low voltage of photovoltaic cells to the high voltage required by the grid [12,13].

In the proposed step-up converter, in addition to providing zero current switching, the voltage stress on the switches is also reduced due to the high voltage gain of the converter, and as a result, switches with lower drain-source resistance and cheaper prices can be used. The auxiliary circuit of the converter also has minimal elements, and there is no additional switch, so the control circuit of the converter is very simple. Another feature of the converter is the transfer of auxiliary circuit energy to the output. On the other hand, the input current

ripple is very low, which makes it suitable for photovoltaic applications. Briefly, the features of the proposed converter can be stated as follows:
- High voltage gain
- Low input current ripple
- The zero current switching of the switch when it is turned on
- The zero voltage switching condition for the switch when it is turned off
- Not using an additional switch
- Absence of reverse recovery problem in circuit diodes
- Low voltage stress on the switch

1.3. Paper organization and structure

In section 2, the proposed converter circuit is described along with its operation in different situations. Also, voltage gain and stress have been investigated in this section and auxiliary circuit design has been described. In section 3, the simulation results of the converter using PSpice software are introduced. Also, the gain of the converter is compared with the hard switching mode. To show the correctness of the converter design, the practical results are shown in section 4, which confirms the correctness of the converter operation. Finally, the conclusions and suggestions for further research are given in section 5.

2. Proposed Second Order Boost Converter

The schematic of the proposed second-order step-up converter is shown in Fig. 1. To increase the gain, L_2-L_3 coupled inductor and capacitor C are used, and to create soft switching conditions, L_{r1}-L_{r2} resonant coupled inductors, C_r capacitor and D_a auxiliary diode are employed. In fact, the inductor L_{r1} provides zero current conditions for turning on the switch S and capacitor C_r provides zero voltage conditions for turning off the switch. Diodes D_1, D_2, D_o, switch S, and capacitor C_o are also the main elements of the circuit. The inductor L_1 at the input also reduces the ripple of the input current in the converter.

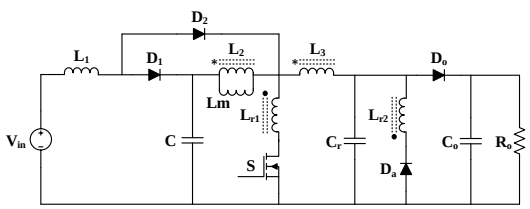

Figure 1. Schematic of the proposed boost converter

2.1. Converter performance statuses

The second-order boost converter has 6 operating states in one switching cycle. Fig. 2 shows the main waveforms of the converter.

For simplicity of analysis, the voltage of capacitors C_o and C is assumed to be constant in one switching cycle because the value of these capacitors is large. Also, due to the large inductors L_1 and L_m, the input current and magnetizing current are assumed to be constant. Before the first mode, the converter switch is off and diodes D_1 and D_o are on and energy is transferred from the input to the output.

Fig. 3 shows the six operation modes of the proposed converter in different time intervals. In this section, the converter performance in different situations is briefly reviewed.

(a) First situation ($t_0<t<t_1$): In this case, the switch S is turned on and due to the series inductor L_{r1} with it, its current increases linearly, because the constant output voltage drops on L_3 and L_{r1} and ZCS condition is provided for switch S. Also, the current of D_1 is reduced and the current of D_2 is increased, until finally the current of D_1 is transferred to D_2. When the current S reaches the I_{Lm} value, this state ends.

$$I_S(t) = \frac{v_o + v_{L3}}{L_{r1}}(t - t_o) \quad (1)$$

(b) Second situation ($t_1<t<t_2$): When the switch current reaches I_{Lm}, the output diode D_o is turned off under the ZC condition, and this state begins. A resonance of L_{r1} and C_r has occurred and the C_r capacitor is discharged. On the other hand, when diode D_2 is turned on, the current of the switch becomes equal to the current of $I_{in}+I_{Lm}$.

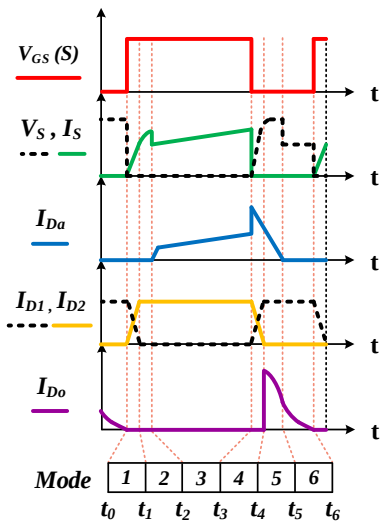

Figure 2. Main waveforms of the boost converter

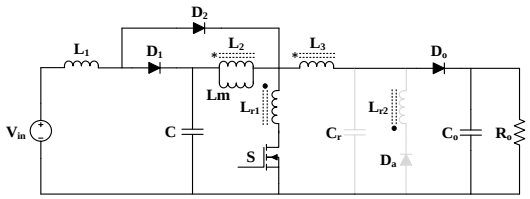

(a) First state ($t_0<t<t_1$)

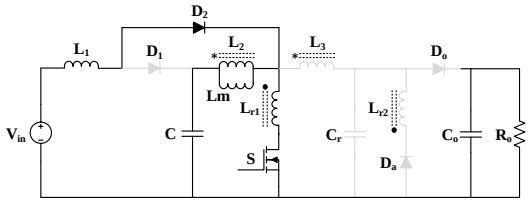

(b) Second state ($t_1<t<t_2$)

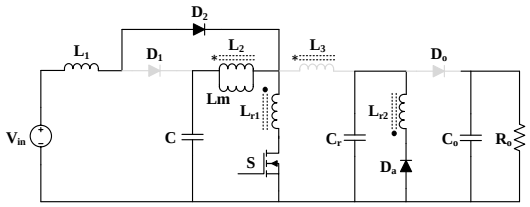

(c) Third situation ($t_2<t<t_3$)

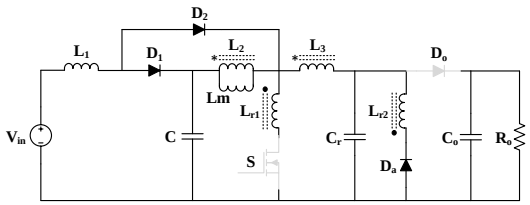

(d) Fourth situation ($t_3<t<t_4$)

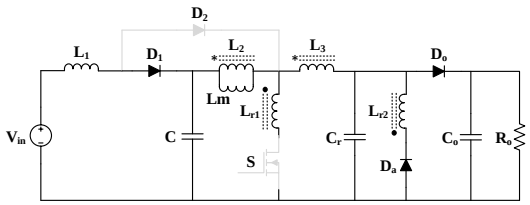

(e) Fifth situation ($t_4<t<t_5$)

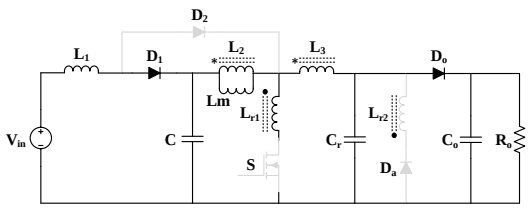

(f) Sixth situation ($t_5<t<t_6$)

Figure 3. The operation modes of the proposed converter at different intervals

(c)Third situation: In this interval, the switch current is constant, equal to the sum of the input current and the magnetizing current, and diodes Do and D_1 are off. Capacitor C charges the magnetizing inductor, and the load current is supplied by the output capacitor. This situation ends when switch S is turned off.

(d) Fourth situation: As the auxiliary diode turns off, D_a is turned on and the energy of L_{r1} is transferred to L_{r2}. Also, the capacitor C_r is charged by the inductor L_3 and auxiliary inductor L_{r2}. Therefore, the switch turns off as ZV. In this interval, the current of D_2 is transferred to D_1.

(e) Fifth situation: In this situation, D_1 is on and D_2 is off. The input current has charged the capacitor C, and the inductor L_m is transferred to the output through L_3 and the output diode D_o. It should be mentioned that the D_o diode conducts as ZV due to the presence of the C_r capacitor. The voltage of C_r capacitor is also clamped at V_o level in this situation.

(f) Sixth situation: When the energy of L_{r2} is exhausted, the diode D_a is turned off, and the voltage across the switch decreases. In this situation, the auxiliary circuit is completely removed from the converter, and the energy of the magnetizing inductor is discharged at the output. This situation ends when the switch is turned on.

2.2. Converter gain

To calculate the voltage-gain of the converter, first the volt-second balance is considered for the input inductor, and then KVL is expressed in the output loop, to obtain the gain of the converter.

2.3. Switch and diode voltage stress

The voltage stress of semiconductor elements is obtained by writing KVL in the loop of the element when it is off.

$$V_{sw} = \frac{V_{in}}{(1-D)^2} = \frac{V_o}{1+nD} = (1+\frac{1}{m}) \quad (2)$$

$$V_{D1} = V_{D2} = V_C = \frac{V_{in}}{1-D} = \frac{V_o(1-D)}{1+nD} \quad (3)$$

$$V_{Do} = nV_C + V_O = \frac{(n+1)V_o}{1+nD} \quad (4)$$

Fig. 4 shows the voltage gain with various duty cycle. As it is clear from Figure 4, the voltage-gain, up to the duty cycle of 0.7 has an almost linear behaviour and from the duty factor of 0.5 to 0.7, the voltage gain becomes four times. Therefore, the dynamic behaviour of the converter is suitable. Fig. 5 shows the normalized voltage stress of semiconductor elements in terms of duty cycle changes where turn ratio is one. As it can be seen from the mentioned figure, with the increase of the duty cycle, the

voltage stress of all the elements has decreased, therefore, increasing both duty cycle and turn ratio can decrease the voltage stress of the elements, which is an advantage compared to other converters.

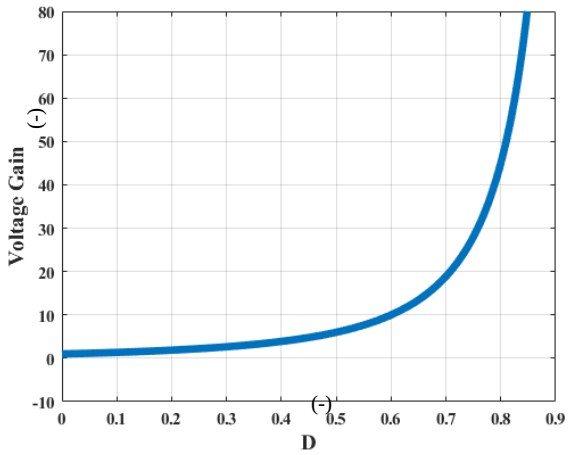

Figure 4. Proposed converter gain versus duty cycle variations

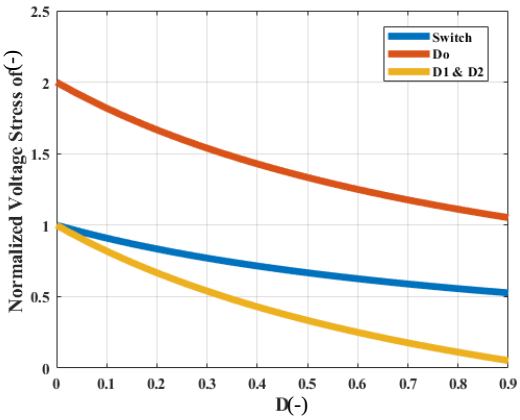

Figure 5. The normalized voltage stress of the proposed converter semiconductor elements versus the duty cycle variations

2.4. Design of auxiliary circuit elements

If t_f is the current falling time, I_{sw} is the switch current before turning off and V_{sw} is the switch voltage after turning off, the snubber capacitor relationship according to (5) is used to design the Cr capacitor.

$$C_r > C_{r\,min} = \frac{I_{sw}\, t_f}{Z V_{sw}} \tag{5}$$

To design the L_{r1} inductor, the snubber inductor relationship according to (6), where t_r is the rise time of the current, is used.

$$L_{r1} > L_{r\,min} = \frac{V_{sw}\, t_r}{I_{sw}} \tag{6}$$

The value of the inductor L_{r1} is obtained from (7), where m is the coupling factor of the auxiliary coupled inductors. The larger m causes the lower the voltage stress of the switch, but the voltage stress of the auxiliary diode increases.

$$L_{r2} = m^2 L_{r1} \tag{7}$$

3. Simulation Results

3.1. Converter circuit in PSPICE software

The proposed step-up converter is designed and simulated by PSPICE software to confirm the theoretical analysis. The circuit schematic of the simulated converter is shown in Fig. 5. The specifications of the converter elements are given in Tables 1 and 2. The design of the converter is done with an input voltage of 40V and an output voltage of 400V under a switching frequency of 100 kHz.

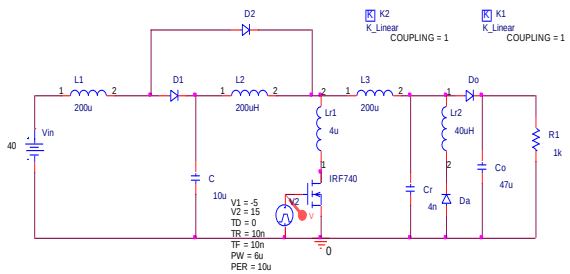

Figure 6. Schematic of the proposed converter simulated in PSPICE

Table 1. Important characteristics of the proposed converter

Parameter	Symbol	Specifications
Main switch	S	IRF740
Circuit diodes	D_1, D_2, D_a, D_o	MUR860

Table 2. Values of the design elements of the proposed converter

Parameter	Symbol	Value
Input voltage	V_{in}	40 V
Output voltage	V_{out}	400 V
Conversion ratio of inductors	n ; m	1:2
Output power	P_{out}	80 W
Switching frequency	f_{sw}	100 kHz
Capacitor	C	10 µF
Output capacitor	C_o	47 µF
Snubber capacitor	Cr	4 nF

3.2. Voltage and current are important elements

Fig. 6 shows the gate-source voltage of the switch S. The drain-source voltage waveform and

the switch current are shown in Fig. 7, according to which and in accordance with the theoretical results and due to the presence of the series inductor, the switch current of the converter has increased with a slope and the switching on of the switch is ZCS.

Also, the voltage of the switch at the turn off instance is also increased by slope due to the presence of the snubber capacitor, and the ZVS conditions are available for the switch at turn off instances. As it is clear from Figure 4, the slope of the switch current is due to the input inductor. The larger value of this inductor, causes the lower slope. Also, the voltage ringings on the switch are due to the resonance of the parasitic capacitor of the switch with the leakage inductor of the coupled inductors.

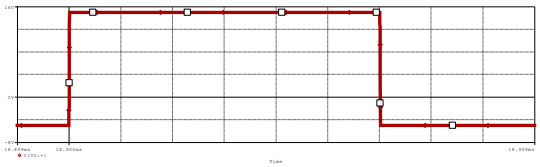

Figure 7. The gate-source waveforms of switch S (4V/div, 1µs/div)

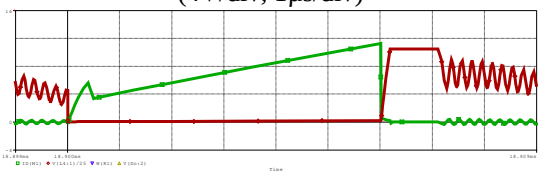

Figure 8. Simulation waveforms of drain-source voltage (red) and current (green) of switch S (4A/div, 100V/div, 1µs/div)

Fig. 8 shows the current waveform of diodes D_1 and D_2, according to which diodes D_1 and D_2 are turned on and off under ZCS conditions. The current of D_a and D_o diodes are shown in Figs. 9 and 10 respectively. It can be seen that the switching on and off of the Da diode was in ZCS condition, and the Do diode was also switched off in ZCS condition because the current has slope. So diodes do not have reverse recovery problem. Therefore, the semiconductor elements of the proposed converter are switched on and off under soft switching conditions.

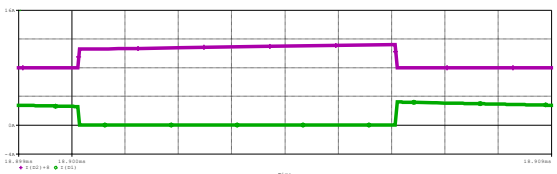

Figure 9. D_1 (top) and D_2 (bottom) diode current simulation waveforms (4A/div, 1µs/div)

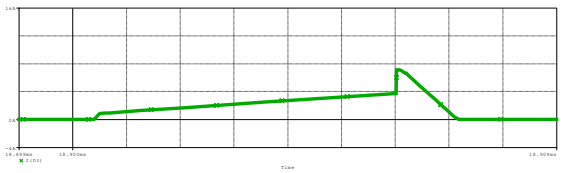

Figure 10. The current simulation waveform of D_a (4A/div, 1µs/div)

Figure 11. The current simulation waveform of D_o (4A/div, 1µs/div)

3.3. Converter efficiency

To investigate the advantages of the proposed converter, the converter efficiency and the hard switching counterpart have been measured. The efficiency diagram of the proposed converter under a 20 W light load to a full load of 80 W is shown in Fig. 11. As can be seen, the efficiency of the proposed converter is 95.50% at full load, which is increased by 5% compared to the hard switching counterpart.

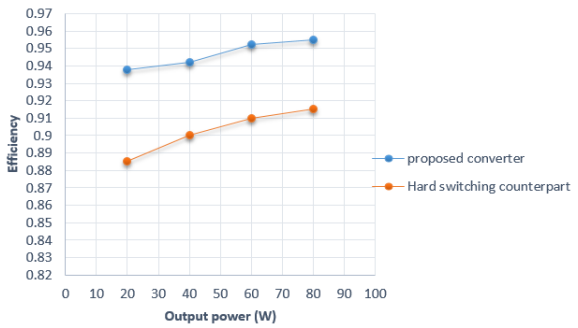

Figure 12. Comparing the efficiency of the proposed converter and the hard switched counterpart

4. Experimental Results

In this section, a prototype of the proposed converter is implemented to prove the simulation results. Fig. 12 shows the implemented converter. Fig. 13 shows the practical waveforms of the switch and converter diodes. As can be seen, the practical results confirm the simulation results.

In Fig (14-a), the slope of the current and voltage at the time of switch on and off shows the ZC and ZV conditions for turning on and off respectively.

On the other hand, according to Fig. (14-b), the current of circuit diodes also decreases with a slope, which indicates the ZC condition when they are turned off. In Figure 14c, the current slope of D_1 and D_2 diodes is greater than the simulation results, which is due to the parasitic inductance of the diodes.

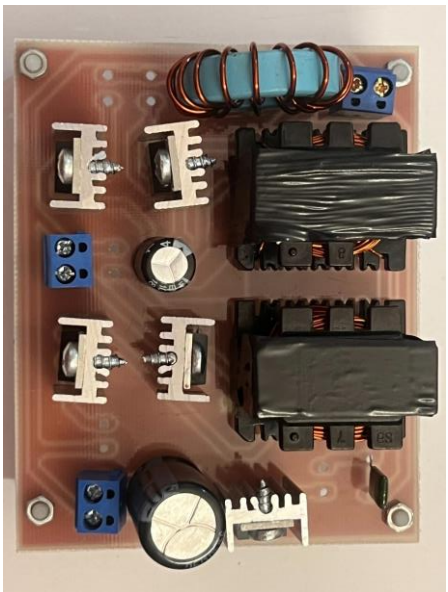

Figure 13. View of the converter made in the laboratory

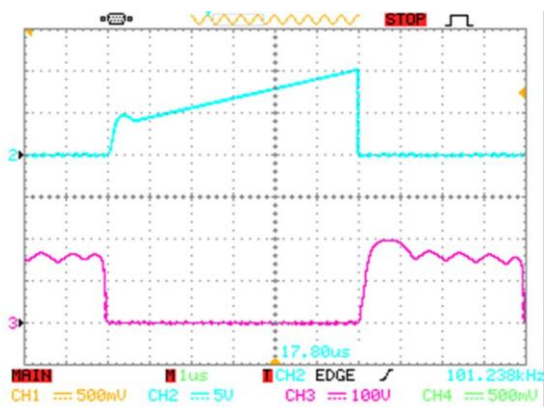

(a) Switch voltage (bottom) and current (up) (5A/div, 100V/div, 1μs/div)

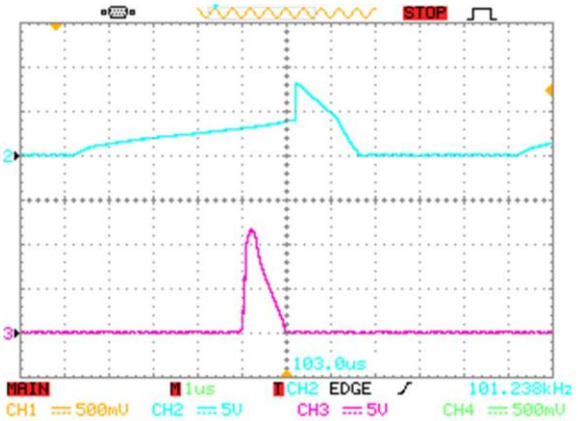

(b) The current of diodes D_o(bottom) and Da(up) (4A/div, 1μs/div)

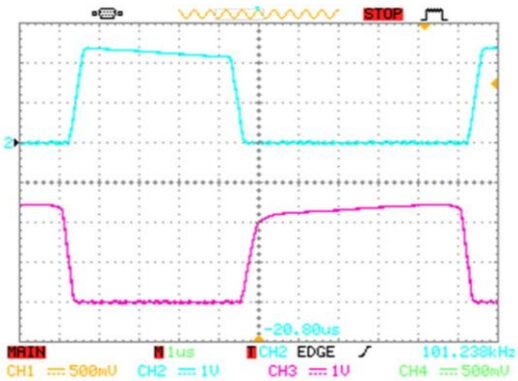

(c) The current of diodes D_1 (up) and D_2 (bottom) (4A/div, 1μs/div)

Figure 14. The measured waveforms of the proposed converter showed by the oscilloscope

5. Comparison of the proposed converter with previous similar converters

Table 3 has been prepared in order to compare the proposed converter with other high step-up converters. As it is clear from the table, the voltage gain of the proposed converter is greater than converters [21] and [25]. Also, the number of elements of the proposed converter is less than converter [21]. The switching conditions in the converters [21-25] are hard switching which causes a significant increase in power losses.

Table 3. Comparison of the proposed converter with previous similar converters

converter	Switching frequency (kHz)	Switching condition	Voltage gain	Voltage stress
[21]	40	Hard	$\frac{4+(2n(1-D))}{1-D}$	$\frac{V_o}{4+n(2-D)-D}$
[22]	100	Hard	$\frac{3+2n}{1-D}$	$\frac{V_o}{3+2n}$

[25]	50	Hard	$\frac{2+nD}{1-D}$	$\frac{V_{in}}{1-D}$
Proposed converter	100	Soft	$\frac{1+nD}{(1-D)^2}$	$\frac{V_o}{1+nD}$

Also, due to the low frequency of the converters [21] and [25], the volume of passive elements of the converter is increased and causing an increase in volume and decrease in the power density of the converters.

6. Conclusions

Considering the low output voltage of solar cells, the utilization of step-up converters becomes necessary to elevate the voltage to the appropriate level required by grid inverters. Various voltage increasing techniques, such as switched capacitors, coupled inductors, diode-capacitor multipliers, or their combinations, are commonly employed. These methods offer a solution to the high duty cycle problem encountered in conventional boost converters. While using a coupled inductor is a common approach to achieve high conversion ratios, it leads to voltage spikes across the switch due to the energy of the resulting leakage inductor. Moreover, converters based on coupled inductors are unsuitable for photovoltaic systems connected to the grid due to the pulse input current, which reduces cell lifespan and poses challenges in tracking the maximum power point. On the other hand, voltage multiplier circuits like diode capacitor multipliers are suitable for low-power renewable energy applications, as they are cost-effective, lack transformers, provide high voltage conversion ratios, and impose low voltage stress.

Isolated converters employ transformers to enhance voltage conversion. However, the presence of transformers increases weight, volume, losses, and ripple in the input current. Consequently, if isolation is not required, non-isolated converters are more suitable for photovoltaic systems. Additionally, soft switching is of great importance as it enables higher switching frequencies, reduces circuit size and weight, and minimizes losses.

This paper proposes a second-order step-up converter that operates with the switch turning on at zero current condition and transfers snubber energy to the output. As a result, auxiliary circuit losses are minimal and do not adversely affect efficiency. Furthermore, the absence of an additional switch simplifies the control circuit, and since the source switch is grounded, isolation is not necessary for the drive circuit. Notable features of the proposed converter include zero current switching of the main switch during turn-on and zero voltage switching when turned off. Moreover, it eliminates the need for an additional switch, exhibits low input current ripple, and avoids reverse recovery issues in circuit diodes. The converter achieves high voltage gain while maintaining low voltage stress on the switch. Further research is recommended to model the converter, design an optimal control circuit, evaluate the reduction of voltage stress on the output diode, eliminate the coupling inductor in the auxiliary circuit, and address capacitive turn-on losses in the converter switch.

Nomenclature

C	Capacitor
Cr	Snubber capacitor
C_o	Output capacitor
D_1, D_2, D_a, D_o	Circuit diodes
f_{sw}	Switching frequency
I_{Lm}	Magnetizing inductor current
I_{sw}	Switch current
L_{r1}, L_{r2}	Resonant inductors
L_m	Magnetizing inductance
n ; m	Turn ratios of coupled inductor
P_{out}	Output power
V_{out}	Output voltage
t_f	the current falling time
t_r	the current rising time
V_{sw}	Switch voltage
V_{in}	Input voltage
V_{D1}, V_{D2}	Diode voltage of D_1 and D_2

References

[1] D.L. Moral, A. Barrado, M. Sanz, A. Lázaro, C. Fernández, P. Zumel, "Analysis and implementation of the autotransformer forward-

flyback converter applied to photovoltaic systems", Solar Energy, vol. 194, pp. 995-1012, Dec. 2019.

[2] G. Dileep, S.N. Singh, "Maximum power point tracking of solar photovoltaic system using modified perturbation and observation method", Renewable and Sustainable Energy Reviews, vol. 50, pp. 109-129, Oct. 2015.

[3] B. Bhandari, K. T. Lee, C. S. Lee, C. K. Song, R. K. Maskey, S. H. Ahn, "A novel off-grid hybrid power system comprised of solar photovoltaic, wind, and hydro energy sources", Applied Energy, Vol. 133, pp. 236-242, Nov. 2014.

[4] Jafari, H., Vaez-Zadeh, S. (2022). Investigation of a new topology for multilevel inverters fed by photovoltaic system for linear induction motor. Journal of Solar Energy Research, 7(3), 1081-1094.

[5] G. Haghshenas, S.M.M. Mirtalaei, H. Mordmand, G. Shahgholian,"High step-up boost-flyback converter with soft switching for photovoltaic applications", Journal of Circuits, Systems, and Computers, Vol. 28, No. 1, pp. 1-16, Jan. 2019.

[6] M. Forouzesh, Y. Shen, K. Yari, Y. P. Siwakoti, F. Blaabjerg, "High-efficiency high step-up dc–dc converter with dual coupled inductors for grid-connected photovoltaic systems", IEEE Trans. on Power Electronics, vol. 33, no. 7, pp. 5967-5982, July 2018.

[7] F. Belhachat, C. Larbes, "A review of global maximum power point tracking techniques of photovoltaic system under partial shading conditions", Renewable and Sustainable Energy Reviews, vol. 92, pp. 513-553, Sept. 2018.

[8] A. Kharrazi, V. Sreeram, Y. Mishra, "Assessment techniques of the impact of grid-tied rooftop photovoltaic generation on the power quality of low voltage distribution network-A review", Renewable and Sustainable Energy Reviews, Vol. 120, Article 109643, March 2020.

[9] M. Abbasi, M. Nafar, M. Simab, "Management and control of microgrids connected to three-phase network with the approach of activating current limitation under unbalanced errors using fuzzy intelligent method with the presence of battery, wind, photovoltaic and diesel sources", Journal of Intelligent Procedures in Electrical Technology, vol. 13, no. 49, pp. 55-66, June 2022.

[10] M.J.V. Vazquez, J.M.A. Marquez, F.S. Manzano, "A methodology for optimizing stand-alone PV-system size using parallel-connected dc/dc converters", IEEE Trans. on Industrial Electronics, vol. 55, no. 7, pp. 2664-2673, July 2008.

[11] Zhang, P., Zhang, G., Du, H. (2018). Circulating current suppression of parallel photovoltaic grid-connected converters. IEEE Trans. on Circuits and Systems, 65(0), 1214-1218.

[12] Fang, X., Yang, Q., Yan, W. (2022). Switching matrix enabled optimal topology reconfiguration for maximizing power generation in series–parallel organized photovoltaic systems. IEEE Systems Journal, 16(2), 2765-2775.

[13] Calcabrini, A., Muttillo, M., Weegink, R., Manganiello, P., Zeman, M., Isabella, O. (2021). A fully reconfigurable series-parallel photovoltaic module for higher energy yields in urban environments. Renewable Energy, 179, 1-11.

[14] Fani, B., Bisheh, H., Sadeghkhani, I. (2018). A protection coordination scheme for distribution networks with high penetration of photovoltaic generators. IET Generation, Transmission and Distribution, 12(8), 1802-1814.

[15] Hajimohammadi, F., Fani, B., Sadeghkhani, I. (2020). Fuse saving scheme in highly photovoltaic-integrated distribution networks. International Transactions on Electrical Energy Systems, 30(1), e12148.

[16] Taheri, D., Shahgholian, G., Mirtalaei, M.M. (2022). Analysis, design and implementation of a high step-up multi-port non-isolated converter with coupled inductor and soft switching for photovoltaic applications. IET Generation, Transmission and Distribution, 16(17), 3473-3497.

[17] A. Kianpour, G. Shahgholian, "A floating-output interleaved boost DC–DC converter with high step-up gain", Automatika, Vol. 58, No. 1, pp. 18-26, April 2017.

[18] Nabati, Y., Halvaei Niaser, A., Mohammadi, H. (2022). A new L-C-D cell based non-isolated single switch high step-up dc-dc converter for photovoltaic applications. Journal of Solar Energy Research, *7*(2), 1027-1036.

[19] S. Semeskandeh, M. Hojjat, M. Hosseini-Abardeh, "Improving the efficiency of floating photovoltaic system in the northern part of Iran using a two-stage multi-string inverter", Journal of Intelligent Procedures in Electrical Technology, vol. 15, no. 57, pp. 85-98, June 2024.

[20] D. Lin, X. Li, S. Ding, Y. Du, "Strategy comparison of power ramp rate control for

photovoltaic systems", CPSS Transactions on Power Electronics and Applications, vol. 5, no. 4, pp. 329-341, Dec. 2020.

[21] A.M.S.S. Andrade, L. Schuch, M.L. Silva Martins, "Analysis and design of high-efficiency hybrid high step-up dc–dc converter for distributed PV generation systems", IEEE Trans. on Industrial Electronics, vol. 66, no. 5, pp. 3860-3868, May 2019.

[22] W. Hassan, D. D. -C. Lu and W. Xiao, "Single-Switch High Step-Up DC–DC Converter With Low and Steady Switch Voltage Stress," in IEEE Transactions on Industrial Electronics, vol. 66, no. 12, pp. 9326-9338, Dec. 2019.

[23] N. Patel, N. Gupta, B. C. Babu, "Photovoltaic system operation as DSTATCOM for power quality improvement employing active current control", IET Generation, Transmission and Distribution, vol. 14, no. 17, pp. 3518-3529, Sept. 2020.

[24] C.T. Hsu, T.J. Cheng, H.M. Huang, Y.D. Lee, Y.R. Chang, J.L. Jiang, "Over frequency control of photovoltaic inverters in an island microgrid", Microelectronics Reliability, Vol. 92, pp. 42-54, Jan. 2019.

[25] S.K. Changchien, T.J. Liang, J.F. Chen, L.S. Yang, "Step-up DC–DC converter by coupled inductor and voltage-lift technique", IET Power Electronics, vol. 3, no. 3, pp. 369-378, May 2010, doi: 10.1049/iet-pel.2009.0089

[26] A. Hamidi, S. Golshannavaz, D. Nazarpour, "D-FACTS cooperation in renewable integrated microgrids: A linear multiobjective approach", IEEE Trans. on Sustainable Energy, vol. 10, no. 1, pp. 355-363, Jan. 2019.

[27] R. Ayop, C.W. Tan, "Design of boost converter based on maximum power point resistance for photovoltaic applications", Solar Energy, vol. 160, pp. 322-335, Jan. 2018.

[28] M. Mirtalaee, R. Amani-Nafchi, "Boost high step-up dc/dc converter with coupled inductors and diode-capacitor Technique", Journal of Intelligent Procedures in Electrical Technology, vol. 10, no. 39, pp. 3-12, Dec. 2019.

[29] M. Dhimish, N. Schofield, "Single-switch boost-buck dc-dc converter for industrial fuel cell and photovoltaics applications", International Journal of Hydrogen Energy, vol. 47, no. 2, pp. 1241-1255, Jan. 2022.

[30] O. Abdel-Rahim and H. Wang, "A new high gain DC-DC converter with model-predictive-control based MPPT technique for photovoltaic systems", CPSS Trans. on Power Electronics and Applications, vol. 5, no. 2, pp. 191-200, June 2020.

[31] M. E. Şahin, "A photovoltaic powered electrolysis converter system with maximum power point tracking control", International Journal of Hydrogen Energy, Vol. 45, No. 16, pp. 9293-9304, March 2020.